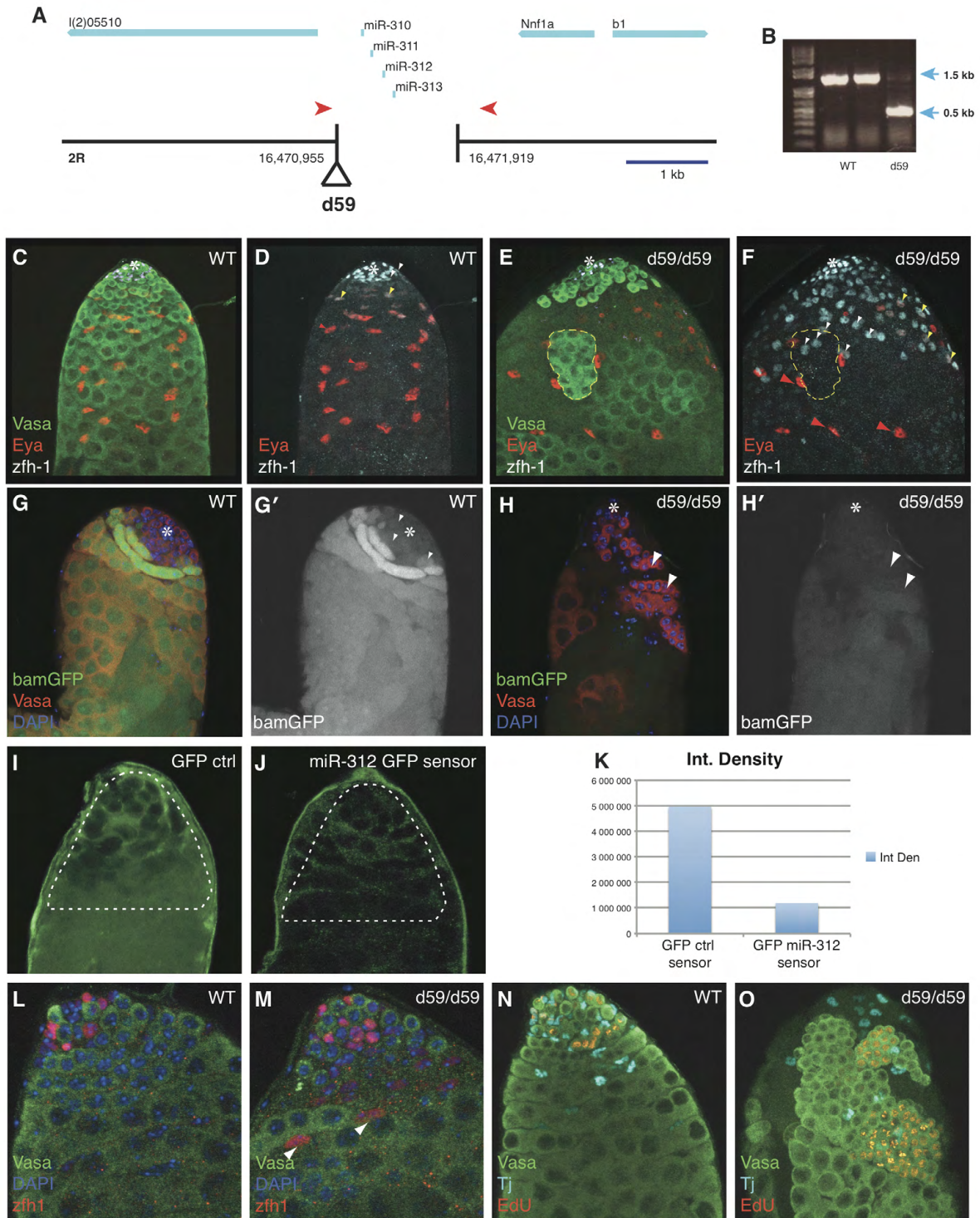
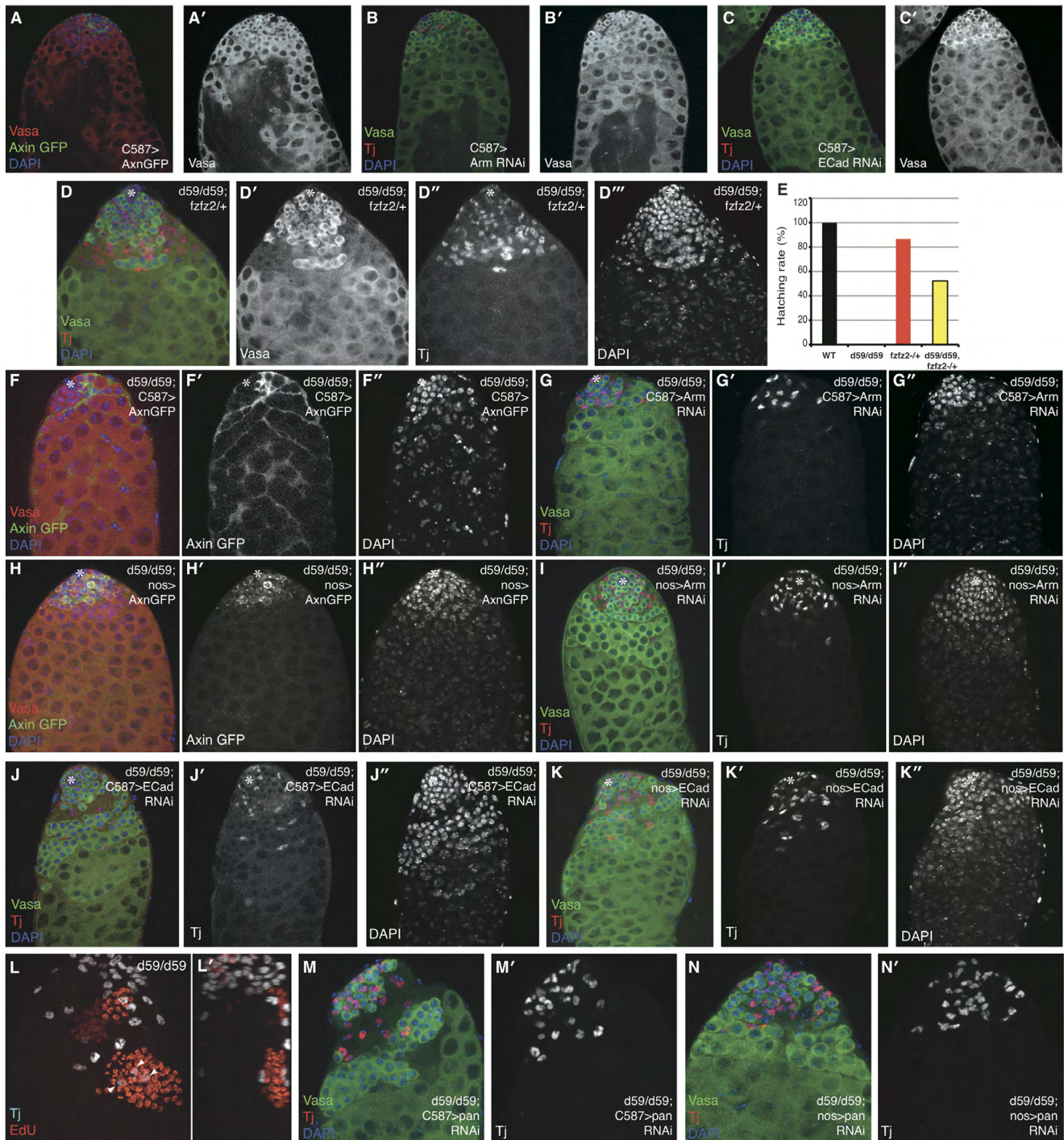


**Fig. S1. Overexpression of miR-310/13 in wing and leg imaginal discs.** Related to Fig. 2. (A-D) Quantification of Dpp-lacZ in imaginal discs in Fig. 3A" (A) and 3B" (B). Integrated fluorescence intensity (FI) quantification of ventral compartment (VC) cells (C), demarcated in A and B by the white dashed line. Integrated fluorescence quantification of dorsal compartment (DC) cells (D), demarcated in A and B by the red dashed line. (E-H) Examples of wild-type imaginal discs (E,F) and imaginal discs overexpressing the miR-310/13 cluster under *ptc*-GAL4 (G,H). Discs overexpressing the miR-310/13 cluster show an expansion of *lacZ* staining into the ventral compartment compared with wild-type discs (green arrowheads). (I,J) Ectopic expression of *Sens* (A) within *Axin*<sup>-/-</sup> MARCM clones positively marked with GFP (yellow arrowheads in J). Note that expression of GFP is not as robust as ectopic expression of *Sens* because of perdurance of the GAL80 inhibitor after recombination, which prevents expression of GAL4-driven UAS-GFP. (K-M') Cells expressing the miR-310/13 cluster inhibit the expression of *Sens* in *Axin*<sup>-/-</sup> MARCM clones. Note that cells expressing high levels of GFP indicate high expression levels of miR-310/13; these cells display a more robust loss of *Sens* compared with cells expressing lower levels of GFP (see white arrows in K-M'). (M') Ratiometric image to quantify the fluorescence intensities of red:green (*Sens*:GFP) channels. Arrows indicate regions of high green and low red, coincident with the loss of *Sens* in cells expressing higher levels of miR-310/13.



**Fig. S2. Generation and characterization of miR-310/13 deletion flies.** Related to Fig. 4. **(A)** EP(2)2586 flies harboring a *P*-element insertion in the vicinity of *mir-310-313* were isogenized and crossed to the D2-3 transposase. The d59 imprecise excision line contained a 1.1 kb deletion that did not affect any of the neighboring genes. Red arrowheads indicate primers utilized to amplify the region depicted in **B**. **(B)** A 1.5 kb region amplified from genomic DNA isolated wild-type flies, whereas d59 flies harbor a 1.1 kb deletion, also confirmed by sequencing. **(C-F)** d59/d59 mutant testes display an increased number of cyst cells expressing the CySCs/early cyst cell marker *Zfh1* (white arrowheads in **F**) compared with wild-type testis (white arrows in **D**). Some of these cells also express low levels of the differentiation marker *Eya* (yellow arrowheads in **F**). Note that cyst cells expressing both markers are also present in wild-type testes (yellow arrowheads in **D**). The abnormal germ cell clusters are engulfed by two or more cyst cells that are *Zfh1*<sup>+</sup> *Eya*<sup>-</sup> (white arrowheads in **F**) or *Zfh1*<sup>-</sup> *Eya*<sup>+</sup> (red arrowheads in **F**), and in some cases *Zfh1*<sup>+</sup> *Eya*<sup>low</sup> (not shown). **(G-H')** d59/d59 testes show little, if any, expression of the differentiation marker *Bam* (white arrowheads in **H,H'**) compared with wild-type testes (**G,G'**). Note that the level of *Bam* staining in D59 testis (**H'**) is similar to that observed in early germ cell progenitors in WT (white arrowheads in **G'**). **(I-K)** Quantification (**K**) of control (**I**) and miR-312 sensor (**J**) tests described in Fig. 4D-E'. **(L,M)** Merged images of *Zfh1* expression in wild-type (shown in Fig. 4H) (**L**) and d59/d59 testes (shown in Fig. 4I) (**M**). **(N,O)** Merged images of *EdU* staining in wild-type (**N**) and d59/d59 (**O**) testes.



**Fig. S3. Genetic interaction studies of *d59/d59* mutant testes.** Related to Fig. 5. (A-C') Testes expressing either Axin-GFP (A,A') or RNAi lines directed against *arm* (B,B') or *E-cad* (C,C') under the C587-GAL4 promoter do not show any discernable phenotypes on their own. (D-D''') Genetic removal of a copy of each of the *fz* and *fz2* genes in the absence of miR-310/13 and the consequent reduction of Arm levels leads to rescue of germ cell clustering and the differentiation phenotype (D') and overall fertility (as shown in E). Note that the phenotype related to somatic cell expansion was not rescued with *fz*, *fz2* removal (D''). (E) Rescue of fertility in *d59/d59* mutants lacking a copy of *fz/fz2*. The hatching rate of embryos laid by WT flies (black), *d59/d59* males crossed to WT females (white), *fz/fz2*<sup>-/-</sup> males crossed to WT females (red) and *d59/d59*; *fz/fz2*<sup>-/+</sup> males crossed to WT females (yellow). All males were aged 24 hours after eclosion and the hatching rate was measured 24 hours after egg deposition. (F-K'') Rescue of germ and somatic cell accumulation phenotype in *d59/d59* flies upon C587-GAL4-driven (soma-specific) expression of Axin (F-F'') or shRNA against *arm* (G-G''). RNAi depletion of E-cad in the soma resulted in a partial rescue (J-J''). Similar observations were made in the germline using the germline-specific *nos*-GAL4 driver to express Axin (H,H''), or shRNAs against *arm* (I-I'') or *E-cad* (K-K''). (L,L') EdU<sup>+</sup> germ cell clusters in *d59/d59* mutants are associated with two or more Tj<sup>+</sup> somatic cells (note three somatic nuclei indicated by white arrowheads in L, and orthogonal view in L'). (M,M') RNAi knockdown of Pan in the somatic lineage using C587-GAL4 in *d59/d59* testes fails to significantly rescue the germ cell clustering/differentiation phenotype as evidenced by the presence of large germ cell clusters (M) and the increased number of Tj<sup>+</sup> cyst cells (M'). (N,N') RNAi knockdown of Pan in the germline using *nos*-GAL4 rescues the germ cell cluster phenotype (N). Note that Tj<sup>+</sup> cyst cell accumulation is not affected by Pan knockdown in the germline (N').

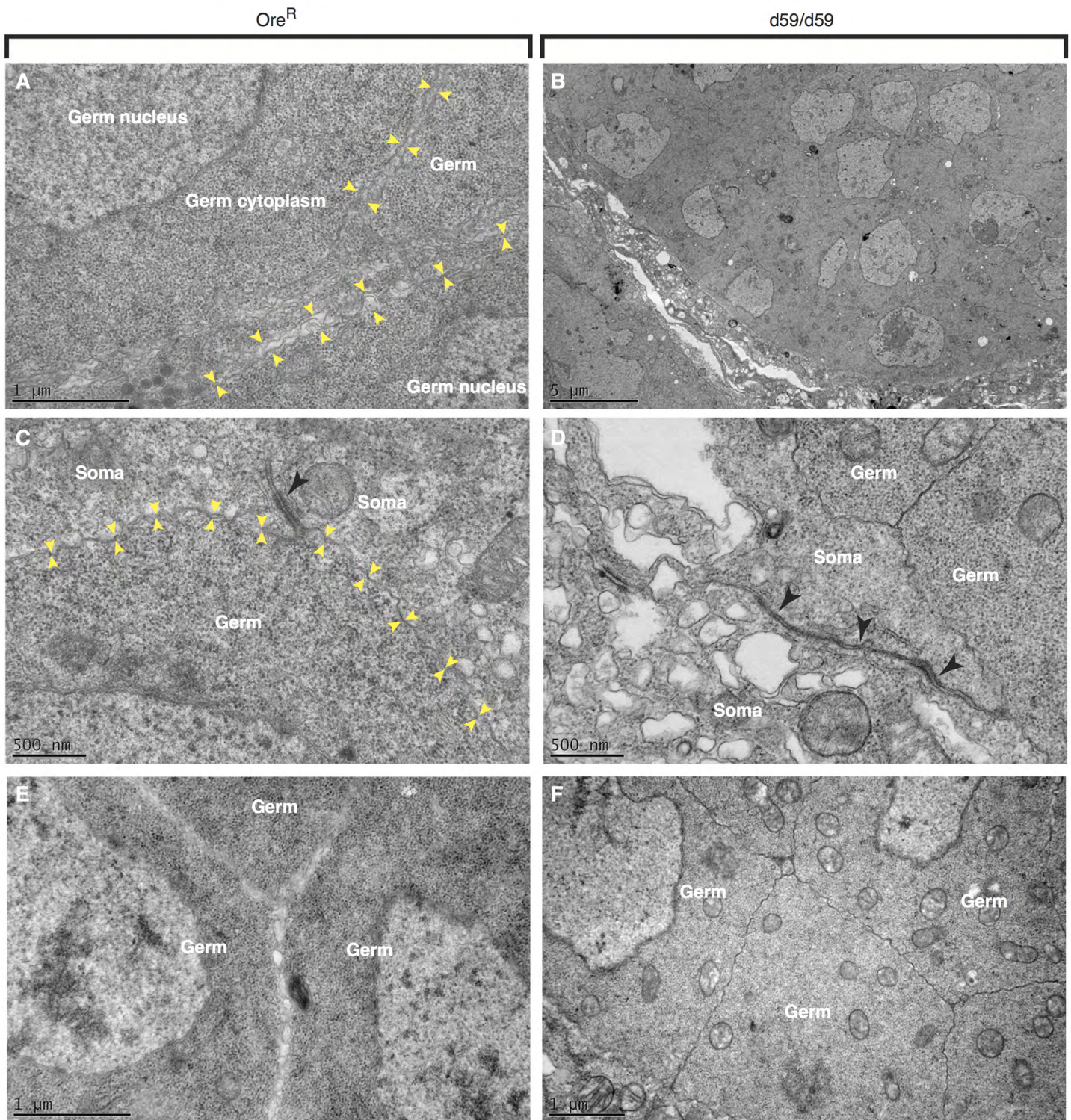


**Fig. S4. Transmission electron microscopy images of WT (*Ore<sup>R</sup>*) and *d59/d59* testes.** Related to Fig. 6. (A) WT testis at 3400 $\times$  magnification. Germ cells are ensheathed by somatic cyst cells. Separation between individual germ cells is visible (yellow arrowheads). (B) *d59/d59* testis germ cell accumulation at 4400 $\times$ . Note the very tight arrangement of germ cells; separation between germ cells is not discernable. (C) Boundary between two cyst cells (labeled Soma) adjacent to a germ cell (labeled Germ) at 40,000 $\times$ . Note the presence of adhesive structure between the somatic cells (black arrowhead). The boundary between germ and somatic cells is indicated by yellow arrowheads. (D) Boundary between two cyst cells (Soma) and two germ cells (Germ) in *d59/d59* testes at 40,000 $\times$ . Note the elongated and extensive electron-dense structure between somatic cells (black arrowheads). (E) WT germ cells at 31,000 $\times$ . Separation between germ cells (Germ) is clearly visible (Y-shaped gap between three germ cells). (F) *d59/d59* mutant germ cells at 19,000 $\times$ . Note the clearly demarcated, electron-dense boundaries between germ cells.

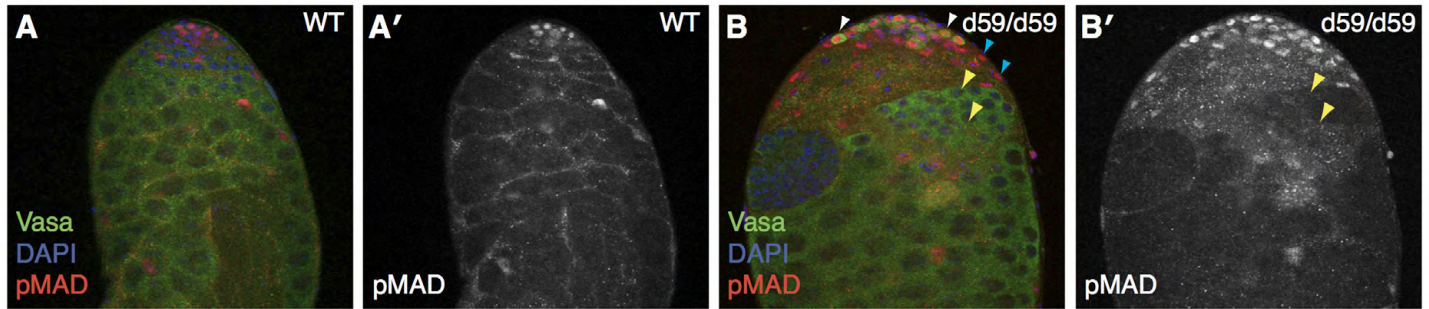


**Fig. S5. Phosphorylated Mad (p-Mad) levels as a readout for TGF $\beta$  signaling.** p-MAD staining in WT (A,A') and d59 mutant (B,B') testes. d59 mutant testes show an increased number of both p-MAD<sup>+</sup> early germ cells (white arrowheads in B) and cyst cells (blue arrowheads in B). p-MAD immunostaining is absent or undetectable in the large abnormal germ cell clusters (yellow arrowheads in B,B';  $n=20$ ).

**Table S1. Primary screen data analysis of Clone 8 cells.** Normalized log scores are shown for each miRNA, as assayed in four replicate experiments.

[Download Table S1](#)

**Table S2. Primary screen data analysis of S2R+ cells.** Normalized log scores are shown for each miRNA, as assayed in four replicate experiments.

[Download Table S2](#)